Technoscience Journal for Community Development in Africa 4 (2025) 177–185
ISSN 2659-0573

Research Article

Iron ore prospecting using remote sensing and aeromagnetic data in parts of sheet 224 (Osi), Nigeria

Bashiru Alaba Ojulari*, Saminu Olatunji, Ismail Oluwaseye Folorunsho

Department of Geophysics, University of Ilorin, Ilorin, Nigeria

Abstract: In recent years, the solid mineral sector has emerged as a central focus of Nigeria's economic diversification agenda, attracting heightened attention from both policymakers and researchers. Iron ore, in particular, is of global economic significance, and its sustainable development has the potential to make substantial contributions to the nation's Gross Domestic Product (GDP). This research applies an integrated exploration strategy that combines remote sensing with aeromagnetic techniques to investigate iron ore mineralisation in parts of Sheet 224 (Osi), located in southwestern Nigeria. Structural analysis reveals that the most prominent lineament orientations trend NNE–SSW (18.52%), NE–SW (17.28%), and ENE–WSW to NW (16.05%). Aeromagnetic data analysis shows prospective mineralisation zones concentrated in the central and northeastern sectors, while enhanced analytical signal values (0.200–0.398) delineate additional target zones primarily situated in the eastern portion of the study area. Spectral depth estimates distinguish two levels of anomalies: shallow sources ranging from 0.06 m to 0.82 m, and deeper sources between 0.40 m and 1.50 m. These results demonstrate that the integration of aeromagnetic datasets with remote sensing imagery provides a reliable framework for identifying subsurface structures and assessing the distribution of iron ore mineralisation.

Keywords: Iron Ore, Remote Sensing, Aeromagnetic

1. Introduction

Over the past decade, Nigeria's push to diversify its economy in order to reduce over dependence on petroleum revenues has refocused policy attention on solid minerals as alternative fiscal anchors (Abudulawal et al., 2017). However, out of thirty-four documented mineral commodities, only about thirteen are presently extracted, processed, and traded—namely coal, kaolin, barite, limestone, dolomite, feldspar, glass sand, small-scale gold, iron ore, lead-zinc, tin, and gypsum (Falade, 2016). Among these, iron ore is especially important. Nigerian iron ore reserves are estimated to exceed 200 million tonnes and could sustain production for more than a century (Okpoli, 2017). Grades range from high (>50% Fe) through medium (30–50% Fe) to low (25–30% Fe), with the highest purities typically associated with basement ridge systems (Filani, 2014). National development initiatives involve the National Iron Ore Mining Company supplying the Ajaokuta Steel Plant and producing super concentrates for the Delta Steel Plant at Aladja near Warri. Despite these endowments, the absence of spatially explicit mineral inventories continues to hinder effective resource development.

Ore formation reflects long-term tectono-geochemical processes. Accordingly, this research used remote sensing and aeromagnetic data analysis for mapping the structural features that channels mineralisation as a reconnaissance tool to identify potential zones of iron ore mineralization in the study area. Remote sensing captures surface characteristics through measured reflected and emitted radiation; its value for mineral exploration has expanded with advances in sensors and processing (Asanbe, 2017). Hence, it offers synoptic multispectral coverage

* Corresponding author
Email: 12-68et003pg@students.unilorin.edu.ng

KWASU PRESS AND PUBLISHING

suitable for mapping lithological boundaries, alteration zones, and structural trends. In addition, analysis of aeromagnetic data provide complementary subsurface information by detecting magnetisation contrasts associated with iron-bearing formations or structurally disrupted basement rocks.

Previous regional studies have used single-dataset approaches—such as Landsat-based structural mapping around Omu-Aran (Asanbe, 2017) and aeromagnetic/ radiometric characterisation of the neighbouring Isanlu Sheet 225 (Akinsunmade et al., 2020). More recent work demonstrates that integrated geospatial analysis provides superior mineral targeting accuracy in Nigerian basement terrains (Adebiyi et al., 2020). The present study builds on these advances by applying a coordinated multisensor workflow that combines remote sensing with aeromagnetic data interpretation to delineate iron-ore occurrences within parts of Sheet 224 (Osi), southwestern Nigeria. The specific objectives are to: (i) extract and quantify dominant structural trends; (ii) produce a Digital Elevation Model (DEM) to support terrain and lineament analysis; (iii) estimate the areal footprint of prospective mineralised zones; and (iv) compute depths to magnetic sources using GIS-supported aeromagnetic techniques.

2. Description of the study area

2.1. Location and accessibility

This research was carried out in southwestern Nigeria within the geographic coordinates of 8°13′0″–8°23′0″ N and 5°00′0″–5°14′0″ E. The study area covers an estimated landmass of approximately 607 km² (Fig. 1). It is well connected by a network of primary and secondary roads. The Ajase Ipo–Omu Aran highway

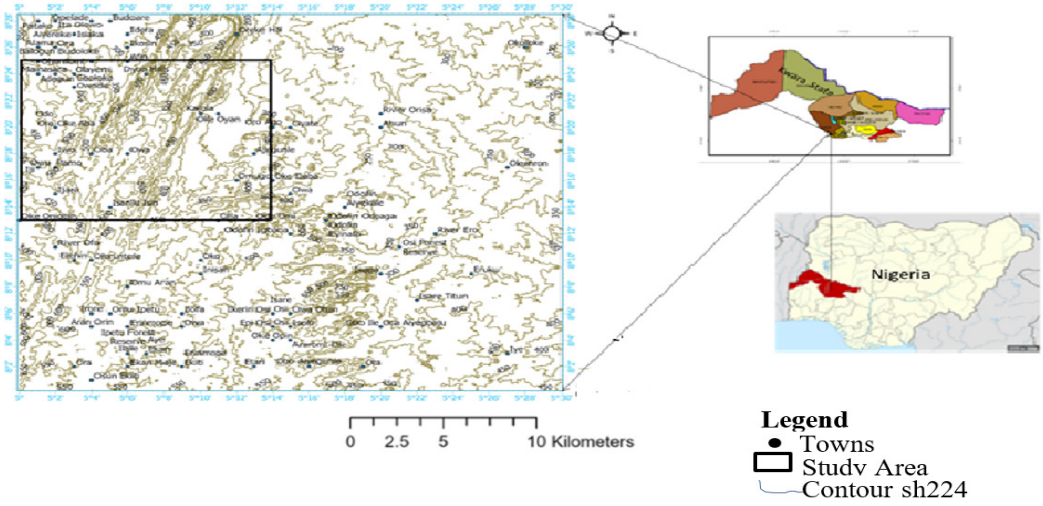

Figure 1: Topographical Map of Sheet 224 (Osi) showing the Study

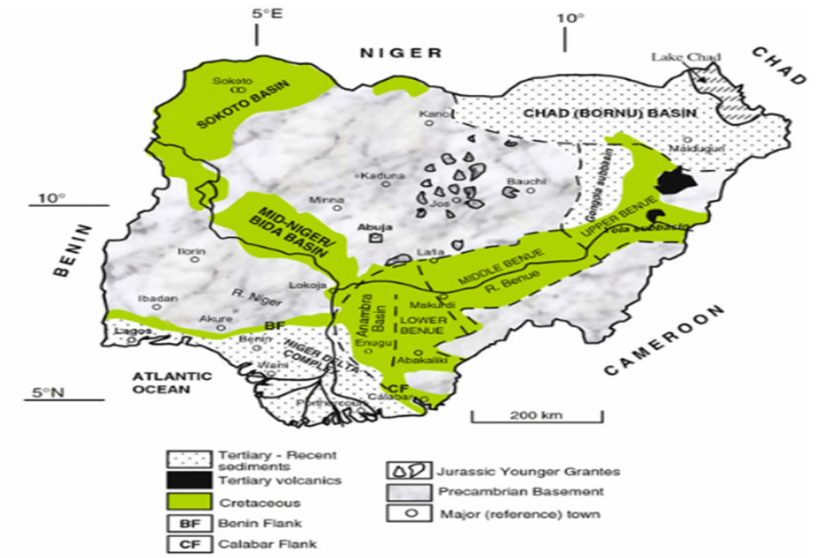

Figure 2: Geological Map of Nigeria Showing the Basement Complex and Sedimentary Basins (Obaje, 2009)

serves as the principal road, while subsidiary roads such as the Oke Onigbin–Owu Isin–Owa Onire and Omu Aran–Olla–Oro Ago–Owa Kajola roads enhance internal accessibility.

2.2. Regional and local geology

The study area lies within the Nigerian Basement Complex, one of the three major litho-petrological divisions of the country (Fig. 2). This crystalline basement forms part of the Pan-African mobile belt situated between the West African and Congo cratons and extending southwards from the Tuareg Shield. Intrusions of the Younger Granites—Mesozoic calc-alkaline ring complexes of the Jos Plateau—occur within the complex, while Cretaceous and younger sediments locally overlie it unconformably.

According to Obaje (2009), the Nigerian Basement Complex preserves the imprint of at least four major orogenic cycles: the Liberian (~2,700 Ma), Eburnean (~2,000 Ma), Kibaran (~1,100 Ma), and Pan-African (~600 Ma) events. Each tectonothermal episode was associated with deformation, metamorphism, and crustal reworking. Consequently, the rocks in the study area display the polycyclic structural characteristics typical of basement terrains across Nigeria, as earlier noted by Rahaman (1988). Recent studies show that the basement rocks record multiple metamorphic and deformational phases, particularly associated with the Eburnean orogeny and Pan-African orogeny, resulting in diverse deformation fabrics and a complex tectono-metamorphic evolution (Ominigbo, 2022).

Also, a reappraisal of the migmatite–gneiss basement in southwestern Nigeria demonstrated marked structural, mineralogical, and petrochemical heterogeneities amongmigmatites, banded gneisses, and granite-gneiss sub-units. Oyinloye (2011) further noted that the area records multiple phases of metamorphism, particularly during the Eburnean and Pan-African cycles, giving rise to a variety of deformation fabrics and complex evolutionary patterns. Field investigations indicate that quartzites and schists dominate the lithology. These rocks are in some places underlain by older gneissic units and intruded by granitoids related to the Pan-African orogeny, as reported by Adedoyin et al. (2013). The study area exhibits a varied physiographic setting, with the local relief largely controlled by a prominent central ridge. Elevations across the terrain range between approximately 450 m and 637 m above sea level, providing moderate topographic highs that define much of the central landscape. In contrast, the lowest elevations occur in the northeastern part, where the land surface descends to about 274 m above sea level, forming a natural depression that influences surface drainage. This altitudinal variation produces gentle to moderately steep slopes, which in turn affect runoff, soil development, and vegetation distribution.

2.3. Climate and Vegetation

Climatically, the region experiences humid tropical conditions, with two distinct seasons that regulate ecological and hydrological processes. The rainy season extends from April to October, while the dry season spans November to March. Mean annual temperatures range between 30 °C and 35 °C, reflecting the typical warm environment of southwestern Nigeria (Olabode & Ajibade, 2010).

Vegetation is dominated by tall grasses, scattered shrubs, and trees, although denser vegetation occurs along river valleys where water availability supports more luxuriant growth. The area functions as an ecotonal transition between the dense rainforest belt of southwestern Nigeria and the Guinea savannah of the north-central zone. Recent studies indicate that vegetation structure and land-cover in these ecotonal zones are strongly influenced by topography, drainage, and human land-use patterns, with evidence of forest degradation and expansion of grassland areas over the last two decades (Akintuyi et al., 2021). Drainage is dendritic in pattern, with several rivers—Orisa, Ofo, Awere, Ogun, Ore, and Arigun—traversing the landscape. River Awere represents the principal channel, flowing in a NE–SW orientation and integrating most of the surface runoff.

3. Materials and methods

3.1. Remote sensing

Shuttle Radar Topography Mission (SRTM) data, with a spatial resolution of 30 m (1 arcsecond), were downloaded from the United States Geological Survey (USGS, 2018). Pre-processing stages include radiometric and geometric corrections followed by PCA, band ratios, decorrelation stretch, and DEM-based hillshading to enhance geological contrasts (Chen et al., 2024). Lineament extraction, performed manually or through edge-detection algorithms, highlights fractures and faults that may channel mineralising fluids. However, remote sensing remains limited by vegetation cover, cloud/cloud-shadow interference, spectral similarity between lithologies, and its inability to image subsurface geometries (Alavipanah, 2022). Using

ArcMap software, two hill-shade images were generated at illumination azimuths of 45° and 135°. Hill-shading is a widely applied visualisation method that enhances topographic expression and facilitates the identification of geomorphic and structural features (Smith & Clark, 2005). Lineaments, comprising both linear and curvilinear features, were automatically extracted from the hill-shade images using the LINE module of PCI Geomatica. This algorithm identifies features based on six threshold parameters—filter radius, edge gradient, curve length, fitting error, angular difference, and linking distance—which were systematically varied until optimal results were obtained (Clark & Wilson, 1994). The adopted parameter values are summarised in Table 1. However, at 30 m resolution, fine-scale terrain variations linked to narrow mineralized zones are often smoothed and may not appear clearly in the elevation model (Farr et al., 2007). Employing multiple illumination directions enhanced the visibility of structural patterns, as single-source shading may obscure some features (Drury, 2001). The density of extracted lineaments was further assessed using the lineament density filter, which acts as an automatic gain control to normalise strong and weak anomalies, thereby improving edge detection and enhancing the interpretation of structural discontinuities (Verduzco et al., 2004). A rose diagram was then used to analyse the orientation of mapped lineaments. Rose plots provide a statistical representation of structural trends such as fractures and faults by showing the distribution of azimuths (Moore et al., 2000). The diagrams were generated using Grapher 8.0 software, enabling the assessment of regional structural alignments. Additionally, a digital elevation model (DEM) was constructed to examine how basement structures influence surface relief. Coloured DEM visualisations have been demonstrated to aid in identifying subtle geomorphic signatures of underlying structures (Adebiyi et al., 2020).

3.2. Aeromagnetic data

Complementary aeromagnetic data were sourced from the Nigerian Geological Survey Agency (NGSA, 2010). These data were collected during a nationwide airborne geophysical survey (2003–2012) conducted by Fugro Airborne Surveys. The survey employed three Scintrex CS3 Cesium Vapor magnetometers, with a flight line spacing of 500 m, tie line spacing of 2000 m, terrain clearance of 80 m, and average flight speed between 250 and 290 km/h. Flight lines were oriented NW–SE, with tie lines flown NE–SW (Tables 2 and 3). A 500 m flight spacing may overlook short-wavelength magnetic responses from small or shallow ore bodies, since widely spaced lines reduce the survey's ability to capture localized anomalies (Nabighian et al., 2005; Hinze et al., 2013).

Table 1: Utilized parameters for the automatic lineament extraction procedure.

Parameter	RADI	GTHR	LTHR	FTHR	ATHR	DTHR
	10	100	100	30	2	5

Table 2: Airborne Geophysical Survey Equipment

Magnetometers	3 x Scintrex CS3 Cesium Vapor
Data Acquisition System	FASDAS
Magnetic Counter	FASDAS
Radar Altimeter	KING KR405/KING KR405B
Barometric Altimeter	ENVIRO BARO/DIGIQUARTZ
Aircraft Supply	Fugro Airborne Surveys
Aircrafts	Cessna Caravan 208B ZS-FSA Cessna Caravan 208 ZS-MSJ Cessna 406 ZS-SSC

Table 3: Airborne Geophysical Survey Parameters (NGSA, 2003)

Survey Parameter	Parameter Specification
Period	2007
Travel line spacing	500 m
Travel line direction	NW – SE
Tie–Line Spacing	5000 m
Tie–Line direction	NE – SW
Nominal Terrain Clearance	80 m
Navigation System	Global Positioning
Sampling Time Radiometric (or less)	0.1 s Magnetic, 0.1 s
Air Speed (Nominal) m/s)	250 – 290 km/hr (70-80
Measurement Spacing (Rad)	8 m (magnetic), 80 m
Flight Line Trend	135 degrees
Tie Line Trend	45 degrees

Data corrections included diurnal variation removal and International Geomagnetic Reference Field (IGRF) adjustment, after which the dataset was micro-levelled to eliminate residual noise. Data processing and enhancement were performed in Geosoft Oasis Montaj (v8.4). Regional–residual separation was achieved using trend-surface analysis, which isolates shallow crustal anomalies by subtracting a polynomial surface representing the regional field from the observed total magnetic intensity (Paterson & Reeves, 1985). Residual

anomalies were interpolated using a 125 m grid cell. Further enhancements included reduction to the equator (Baranov and Naudy, 1964), analytic signal computation (Roest et al., 1992), and source parameter imaging (Thurston & Smith, 1997). These transformations improved the delineation of structural features such as faults, shear zones, and intrusive contacts, thereby strengthening the integration of aeromagnetic and remote sensing interpretations. Depth-to-source estimation was done using spectral analysis aids interpretation of magnetic body geometry. Nonetheless, aeromagnetic interpretation is inherently non-unique, and resolution is constrained by survey line spacing, sensor altitude, magnetic noise, and weak susceptibility contrasts; remanent magnetisation and deep weathering may further obscure anomalies.

4. Results and discussion

4.1. Remote sensing

The lineament density map (Fig. 3) reveals that the short-wavelength anomalies are predominantly linear to elliptical, reflecting shear deformation oriented NE–SW and expressed as faults, fractures, and lithological contacts. These structures are significant because iron-ore systems in basement terrains are commonly structurally controlled, with shear zones and fracture networks acting as conduits for Fe-rich hydrothermal fluids (Bierlein et al., 2006; Holden et al., 2008; Umar et al., 2024). The elongation of hills along this dominant structural trend further supports the role of tectonic deformation in creating favorable pathways for mineralization.

The major surface lineaments also align with the trend of volcanic units in the region, where valleys preferentially exploit zones of structural weakness nearly parallel to the NE–SW and NW–SE shear systems. Such structurally prepared corridors are widely documented as key targets in iron-ore exploration due to their propensity to concentrate mineralizing fluids and enhance ore deposition (Akinlalu et al., 2025; Porwal et al., 2006).Lineament trend analysis using the rose diagram (Fig. 4) identifies four dominant orientations—NNE–SSW, NE–SW, NW–SE, and ENE–WSW—with the NE–SW trend accounting for the highest proportion (18.52%). The significance of this orientation lies in its coincidence with major regional shear zones known to localize iron-ore bodies in the Nigerian Basement Complex and related terranes (Umar et al., 2024). The supporting minor orientations (N–S, NNW–SSE, WNW–ESE, and E–W) collectively suggest a multiply deformed crustal block in which cross-structures may enhance fluid flow and promote ore concentration.

The coloured digital elevation model (DEM) generated from SRTM data (Fig. 5) highlights topographic variation consistent with active or inherited tectonism. A NE–SW-trending ridge occupies the central portion of the area, with elevations of 527–637 m, interpreted as a compressional feature or monocline. Such uplift and associated displacement can create permeability contrasts that focus hydrothermal circulation—an important mechanism in basement-hosted iron-ore mineralization (Akinlalu et al., 2025). The pronounced topographic gradients between the ridge and the lower-lying northeastern terrain (224–323 m) further support the influence of crustal deformation in creating structural traps and depositional environments favourable for Fe-ore concentration.

4.2. Aeromagnetic data

The Total Magnetic Intensity (TMI) map (Fig. 6) reveals a prominent zone of low magnetic anomalies, ranging from 32,948.5 nT to 32,050.0 nT, which dominates the northeastern portion of the study area. A similar low anomaly trend extends centrally in a NE–SW orientation. Intermediate magnetic intensities, between 32,969.9 nT and 32,951.1 nT, occur in the northwestern sector, while the highest TMI values (32,969.9 nT to 33,040.8 nT) are concentrated in the southwestern and southeastern portions of the area.

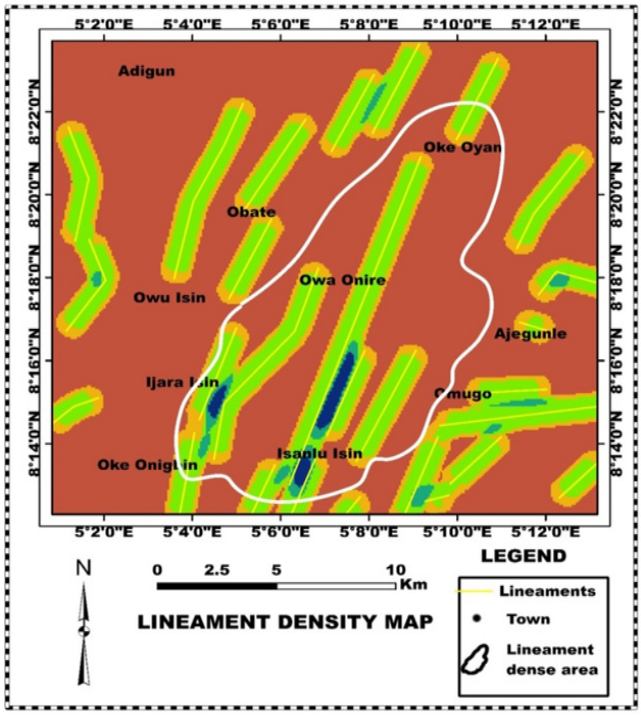

Figure 3: Lineament Density Map of the Study Area

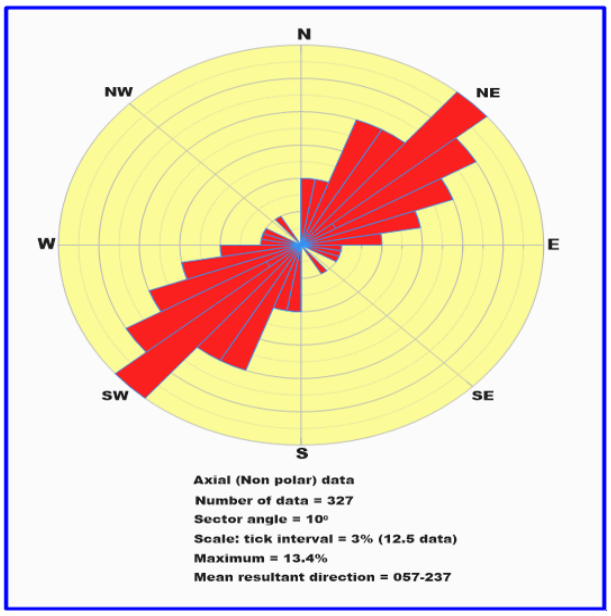

Figure 4: Rose Diagram of the Study Area

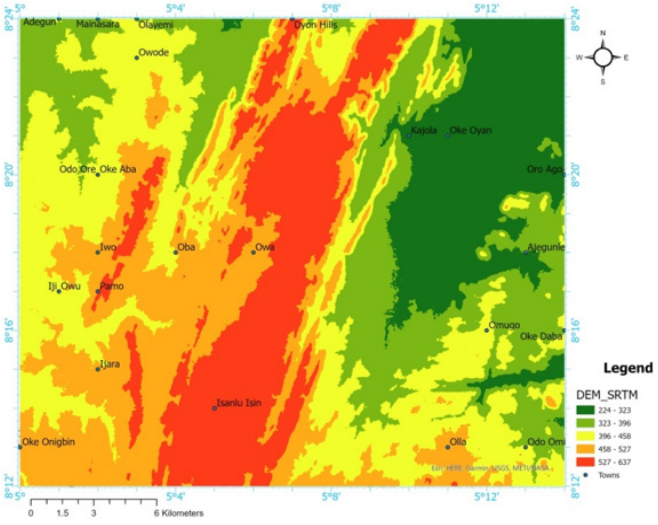

Figure 5: Digital Elevation Model (DEM) of the Study Area

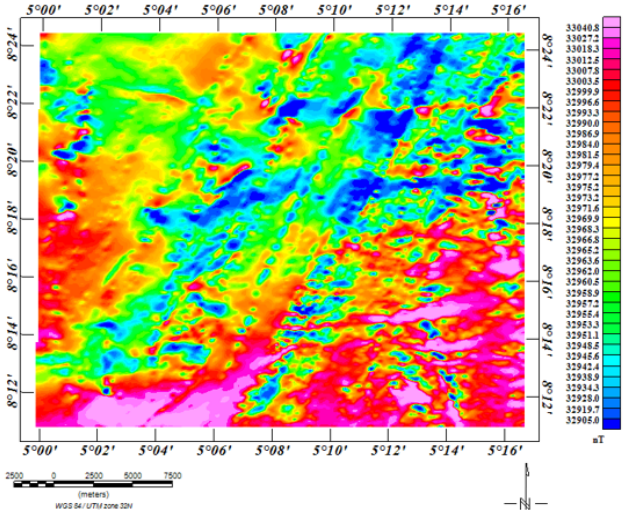

Figure 6: Total Magnetic Field (TMI) Map of the Study Area

The residual magnetic field map (Fig. 7) highlights maximum magnetic field strengths ranging between 4.8 nT and 75.9 nT in the southwest and southeast, while the northwestern and northeastern sectors exhibit relatively weaker intensities, spanning from 4.8 nT to –21.9 nT (low) and –27.6 nT to –84.4 nT (intermediate), respectively. These results suggest that the regional magnetic field (Fig. 6) is significantly stronger than the residual field (Fig. 7), with the residual anomalies reflecting relatively shallow magnetic sources. Since the amplitude of magnetic anomalies is proportional to rock magnetization, which depends on magnetic susceptibility (Gunn et al., 1997), the residual anomalies provide important insights into lithological contrasts. In low magnetic latitude regions, such as Nigeria, anomalies are inverted: rocks with low magnetic susceptibility often generate high magnetic responses, whereas highly susceptible rocks may appear as low anomalies (Gunn et al., 1997). Accordingly, the residual magnetic image (Fig. 7) indicates that high susceptibility zones—displayed as low magnetic intensities (blue)—are concentrated in the northeastern and central portions of the study area, suggesting the presence of iron ore mineralization. Conversely, low-susceptibility rocks, such as schists and quartzites, are represented by high magnetic values (pink) in the southwest and southeast.

To correct for Nigeria's location near the magnetic equator, the total field intensity map (Fig. 6) was reduced to the equator (RTE) (Fig. 8). The RTE transformation delineates three distinct magnetic zones across the study area. High-intensity anomalies (32,973.7 nT to 33,045.6 nT) dominate the southwestern and southeastern portions, whereas low anomalies (32,968.1 nT to 32,952.8 nT and 32,944.2 nT to 32,910.9 nT) are identified in the northwestern and southwestern regions. These low RTE anomalies are spatially correlated with known iron ore deposits at Itakpe, Choko Choko, Obajana, Ajanbanoko, and Kakun (Faruwa et al., 2021). Such anomalies are of considerable economic significance, as in low-latitude settings, positive magnetic susceptibility sources typically manifest as magnetic lows (Amigun et al., 2015; Ojo, 1990). The structural elongation of these anomalies suggests fault-controlled emplacement along NE–SW trending shear systems, which likely exert a first-order control on ore localisation.

The analytical signal map (Fig. 9) provides a direct measure of the magnetic anomaly intensity, allowing for more precise delineation of contacts, edges, and lithological boundaries within the study area. The lowest signal amplitudes, ranging between 0.0095 nT/m and 0.3441 nT/m, are recorded in the northwestern portion of the area, corresponding to zones likely underlain by

metasedimentary and metavolcanic rocks. In contrast, higher analytical signal amplitudes (0.13–0.43 nT/m) are concentrated in the northeastern and southeastern sectors, with anomalies trending predominantly in the NE–SW direction.

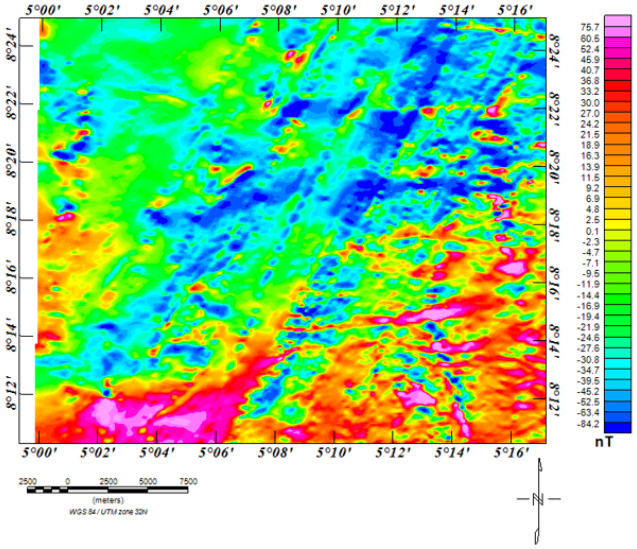

Figure 7: Residual Magnetic Field Intensity Map of the Study Area

These elevated amplitudes are associated with magnetic sources dominated by rocks of the meta-sedimentary complex (MSC), which have been previously recognized as hosts to mineralization in similar Nigerian terrains (Amigun et al., 2015).

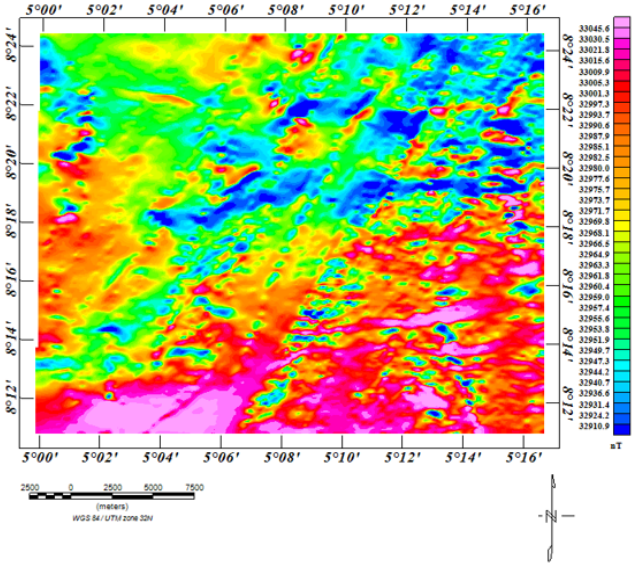

Figure 8: Reduction-to-the-Equator (RTE) Map the Study Area

Depth estimation was conducted using the Source Parameter Imaging (SPI) technique, which provides a reliable means of approximating the depth to the top of magnetic sources. The spectral depth analysis map (Fig. 10) reveals two primary depth domains: shallow sources, ranging from 0.06 m to 0.82 m, and deeper sources, ranging from 0.4 m to 1.5 m. The shallow anomalies are interpreted as representing ironstone occurrences at near-surface levels, while the deeper anomalies likely reflect the top of the magnetic basement. This depth variation suggests a structurally controlled subsurface framework, where mineralized shallow bodies are superimposed on deeper basement structures, consistent with tectono-magmatic processes that facilitated mineral deposition.

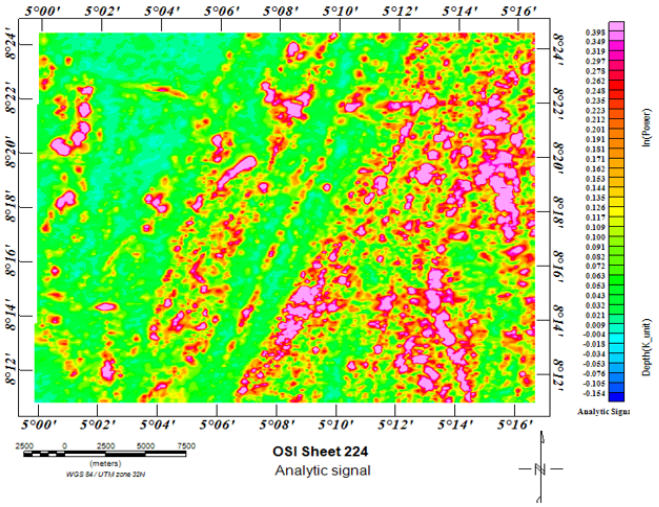

Figure 9: Analytic Signals Map the Study Area

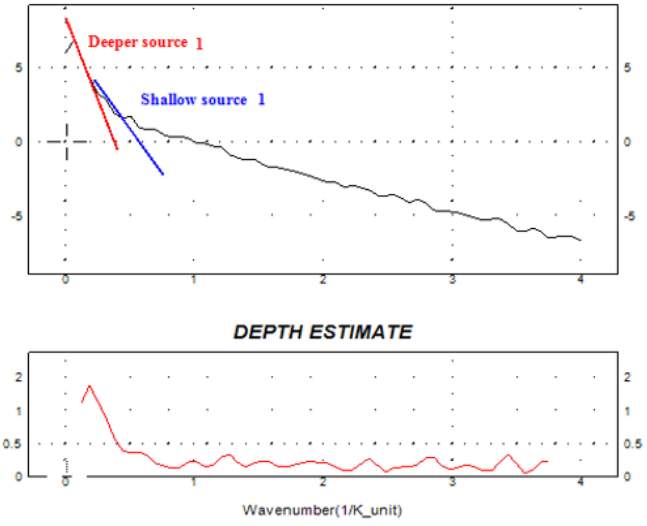

Figure 10: Spectral Depth Analysis Map of the Study Area

5. Conclusion and recommendation

The integrated analysis of remote sensing and aeromagnetic data provides a comprehensive understanding of the structural, lithological, and mineralization framework of the study area. Lineament and DEM analyses reveal dominant NE–SW, NNE–

SSW, ENE–WSW, and NW–SE structural trends, with elevated ridges and low-lying terrains reflecting tectonic influences on both surface and subsurface morphology. Magnetic data, including Total Magnetic Intensity (TMI), residual anomalies, Reduction-to-the-Equator (RTE) outputs, and analytical signal maps, consistently indicate zones of high and low magnetic susceptibility, highlighting prospective iron-ore-bearing formations. Depth estimation using Source Parameter Imaging (SPI) further confirms the presence of shallow ironstone deposits overlying deeper basement structures, demonstrating a structurally and tectono-magmatically controlled mineralization pattern.

Overall, the findings establish that NE–SW trending shear zones act as principal pathways for ore emplacement, with structural intersections and lithological contrasts serving as favorable loci for iron-ore concentration. This integrated geophysical and remote sensing approach not only refines the delineation of lithological contacts and mineralized zones but also provides a practical framework for guiding future iron-ore exploration within the Nigerian basement complex. Consequently, such analyses are essential for enhancing mineral resource development, supporting sustainable exploration, and contributing to Nigeria's broader economic diversification objectives. However, the aeromagnetic and remote sensing have limitations in depth and scope of investigation. Therefore, further detailed geophysical surveys, such as ground magnetic surveys and geochemical studies, are recommended.

6. Acknowledgements

I gratefully acknowledge the respondents for their cooperation and willingness to share their knowledge on medicinal plants used for the treatment of inflammatory disease. I am greatly indebted to the staff of the Forestry Research Institute of Nigeria (FRIN) for the identification of the plants.

References

Abudulawal, L., Amidu, S.A., Adeagbo, O.A. and Adejumo, S.A. (2017) Overburden Thickness and Potential Tonnage Estimate of Olode-Gbayo Pegmatite Deposit, Southwestern Nigeria, Using Electrical Resistivity Method. *Journal of Geography, Environment and Earth Science International 10(2),* 1-12.

Adebiyi, L.S., Fatoba, J.O., Salawu, N.B., Dopamu, K.O., Abdulraheem, T.Y., Obaseki, O.S., Olasunkanmi, N.K., Adediran, S.O. (2020) Analysis of aeromagnetic data: Application to Early-Late Cretaceous events in parts of Lower Benue trough, Southern Nigeria. *Journal of Applied Geophysics 178,* 10405. https://doi.org/10.1016/j.jappgeo.2020.104052.

Adedoyin, A.D., Adekeye, J.I.D., Ojo, O.J., Bamigboye, O.S. and Ajayi, M.T. (2013) Oke-Ode Dome: A Product of Fold Interference Followed By Shearing. *Scottish Journal of Arts, Social Sciences and Scientific Studies 12*(2), 100-107. http://scottishjournal.co.uk.

Akinlalu, A. A., Adabanija, M. A., & Olayinka, A. I. (2025) Structural controls on iron-ore accumulation within basement complex terrains: Implications for exploration targeting. *Journal of African Earth Sciences, 230,* 108123.

Akinsunmade, A., Dinh, C.N. Wojas, A. and Suchoń, S.T. (2020) Characterization of lithological zones of the Isanlu sheet 225, North Central Nigeria, using aerogeophysical datasets *Acta Geophysica, 68,* 651–665 https://doi.org/10.1007/s11600-020-00411-6.

Akintuyi A. O., Fasona M. J., Ayeni A. O. & Soneye A. S. (2021) Land use/land cover and climate change interaction in the derived savannah region of Nigeria, *Environmental Monitoring and Assessment*, *193 (12),* 1–24.

Alavipanah, S. K., Karimi Firozjaei, M., Sedighi, A., Fathololoumi, S., Zare Naghadehi, S., Saleh, S., & M. Atkinson, P. (2022) The shadow effect on surface biophysical variables derived from remote sensing: A review. *Land, 11*, 11

Amigun, J. O., Ojo, S. B., and Afolabi, O. (2015) Interpretation of high-resolution aeromagnetic data over Okene area, Nigeria, for iron ore exploration. *Journal of Applied Geophysics, 120*, 65–75. https://doi.org/10.1016/j.jappgeo.2015.06.009.

Asanbe, O.A. (2017) Structural Geological Mapping of Omu-Aran, Kwara State Using Remote Sensing. Unpublished M.Sc. Thesis, Federal University of Technology, Akure. URI: http://196.220.128.81:8080/xmlui/handle/123456789/1686.

Baranov, V. and Naudy, H. (1964) Numerical calculation of the formula of reduction to the magnetic pole. *Geophysics, 29(1),* 67–79. https://doi.org/10.1190/1.1439334.

Bierlein, F.P., Murphy, F.C., Weinberg, R.F., Lees, T., Craton, Y. (2006) Distribution of orogenic gold deposits in relation to fault zones and gravity gradients : targeting tools applied to the Eastern. *Miner Deposita 41,* 107–126. https://doi.org/10.1007/s00126-005-0044-4.

Chen, Y., Wang, Y., Zhang, F., Dong, Y., Song, Z., & Liu, G. (2023) Remote sensing for lithology mapping in vegetation-covered regions: Methods, challenges, and opportunities. *Minerals, 13(9),* 1153.

Clark, C. D. and Wilson, C. (1994) Spatial analysis of lineaments. *Computers & Geosciences*, *20(7-8),* 1237–1251. https://doi.org/10.1016/0098-3004(94)90073-6.

Drury, S. A. (2001) Image interpretation in geology (3rd ed.). London: Routledge.100-135

Falade, M. (2016) A Profile of Nigeria's Solid Minerals A detailed Desk Review. 10.13140/RG.2.1.4233.9600.

Farr, T. G., Rosen, P. A., Caro, E., Crippen, R., Duren, R., Hensley, S., and Alsdorf, D. (2007) The Shuttle Radar Topography Mission. *Reviews of Geophysics, 45(2),* RG2004. https://doi.org/10.1029/2005RG000183.

Faruwa, O. I., Oladunjoye, M. A. and Ogunbona, I. O. (2021) Geophysical investigation of iron ore deposits using aeromagnetic data in parts of Kogi State, North-Central Nigeria. *Journal of African Earth Sciences, 178*, 104–131. https://doi.org/10.1016/j.jafrearsci.2021.104131.

Filani, A.O. (2014) The Prospects of Solid Minerals Industry in Nigeria. *International Journal of Education and Research*, *2(7),* 689-696.

Gunn, P., Maidment, D., & Milligan, P. (1997) Interpreting aeromagnetic data in areas of limited outcrop. *AGSO Journal of Australian Geology & Geophysics, 17(2),* 175–185.

Hinze, W. J., Von Frese, R. R. B., and Saad, A. H. (2013) Gravity and magnetic exploration: Principles, practices, and applications. Cambridge University Press. 216-266.

Holden, E., Dentith, M., Kovesi, P., (2008) Towards the automated 589 analysis of regional aeromagnetic data to identify regions prospective or gold deposits. *Computers and Geosciences 34,* 1505–1513. https://doi.org/10.1016/j.cageo.2007.08.00.

Moore, D. E., Smith, J. V. and Thurston, J. B. (2000) Application of rose diagrams to structural geology. *Journal of Structural Geology, 22(9),* 1239–1253. https://doi.org/10.1016/S0191-8141(00)00048-2.

Nabighian, M. N., Grauch, V. J. S., Hansen, R. O., LaFehr, T. R., Li, Y., Peirce, J. W., and Shive, P. N. (2005) The historical development of the magnetic method in exploration. *Geophysics, 70(6),* 33–61. https://doi.org/10.1190/1.2133784.

Nigerian Geological Survey Agency (2010) Airborne geophysical survey data acquisition and processing report. Abuja: Federal Ministry of Mines and Steel Development.

Obaje, N.G., (2009) Geology and Mineral Resources of Nigeria, Lecture Notes in Earth Sciences 120, Springer-Verlag Berlin Heidelberg, P221.

Ojo, S. B. (1990) Origin of iron ore deposits of Itakpe area, Kogi State, Nigeria, from aeromagnetic and gravity studies. *Geophysics, 55(6)*, 732–745. https://doi.org/10.1190/1.1442892.

Okpoli, C.C. (2017) Geolectric and geochemical appraisal of Iron-ore deposit: Case study of Akunu-akoko, southwestern Nigeria. *Science and Technology*, *3(11),* 158-180.

Olabode, A.D. and. Ajibade, L.T. (2010) Environment Induced Conflict and Sustainable Development-A Case of Fulani-Farmers' Conflict In Oke-Ero LGA, Kwara State, Nigeria *Journal of Sustainable Development in Africa*,*12(5),* 159-173.

Ominigbo, O. E. (2022) Evolution of the Nigerian basement complex: current status and suggestions for future research. *Journal of mining and Geology*, *58(1),* 229-236.

Oyinloye, A.O. (2011) Beyond Petroleum Resources: Solid Minerals to the rescue: 31st Inaugural Lecture of the University of Ado-Ekiti, Nigeria Press, 1-36.

Paterson, N. R. and Reeves, C. V. (1985) Applications of gravity and magnetic surveys: The state-of-the-art in 1985. *Geophysics,* 50(12), 2558–2594. https://doi.org/10.1190/1.1441886.

Porwal, A., John, E., Carranza, M., Hale, M. (2006) Tectonostratigraphy and base-metal mineralization controls, Aravalli province (western India): New interpretations from geophysicaldata analysis *29,* 287306. https://doi.org/10.1016/j.oregeorev.2005.10.003.

Rahaman MA (1988) Recent advances in the study of the basement complex of Nigeria. In: Geological Survey of Nigeria (ed) *Precambrian Geol Nigeria*, 11–43.

Roest, W. R., Verhoef, J. and Pilkington, M. (1992) Magnetic interpretation using the 3-D analytic signal. *Geophysics*, *57(1),* 116–125. https://doi.org/10.1190/1.1443174.

Smith, M. J. and Clark, C. D. (2005) Methods for the visualisation of digital elevation models for landform mapping. *Earth Surface Processes and Landforms*, 30(7), 885–900. https://doi.org/10.1002/esp.1210.

Thurston, J. B. and Smith, R. S. (1997) Automatic conversion of magnetic data to depth, dip, and susceptibility contrast using the SPI method. *Geophysics*, 62(3), 807–813. https://doi.org/10.1190/1.1444190.

Umar, M. M., Orazulike, D. M., & Yakubu, T. A. (2024) Structural influences on iron ore mineralisation in basement complex terrains of Nigeria. *Journal of African Earth Sciences*, *209,* 105589.

United States Geological Survey (USGS). (2018) Shuttle Radar Topography Mission (SRTM) global data products. Retrieved from https://www.usgs.gov.

Verduzco, B., Fairhead, J. D., Green, C. M. and MacKenzie, C. (2004) New insights into magnetic derivatives for structural mapping. *The Leading Edge*, *23(2)*, 116–119. https://doi.org/10.1190/1.1651454.